Comparative evaluation of PFAS-selective adsorbents in hard-to-treat residual waste streams☆

Ashley Hesterberg Butzlaff [a], Bineyam Mezgebe [a], Ashton Collins [b], Zhi-Wei Lin [c], Dyandra Lassalle-Vega [d], Irene M. Harmody [e], Orlando Coronell [f], Frank A. Leibfarth [e], William R. Dichtel [c], Mallikarjuna Nadagouda [a], Mohamed Ateia [a,g,*]

[a] Center for Environmental Solutions & Emergency Response, US Environmental Protection Agency, Cincinnati, OH, USA
[b] Oak Ridge Associated Universities, US Environmental Protection Agency, Cincinnati, OH, USA
[c] Department of Chemistry, Northwestern University, Evanston, IL 60208, USA
[d] Student Volunteer at Center for Environmental Solutions & Emergency Response, US Environmental Protection Agency, Cincinnati, OH, USA
[e] Department of Chemistry, University of North Carolina, Chapel Hill, NC 27599, USA
[f] Department of Environmental Sciences and Engineering, Gillings School of Public Health, University of North Carolina, Chapel Hill, NC 27599, USA
[g] Department of Chemical and Biomolecular Engineering, Rice University, Houston, TX, USA

ABSTRACT

The removal of per- and polyfluoroalkyl substances (PFAS) in complex waste streams remains an urgent environmental challenge due to their persistence and resistance to conventional treatment methods. This study investigates the performance of five PFAS-selective adsorbents: three cyclodextrin-based polymers, a hydrogel, and a polymer-metal oxide hybrid against traditional granular activated carbon (GAC) and ion exchange (IX) resins. While previous studies have examined PFAS removal in idealized conditions, the performance of these PFAS-selective adsorbents in complex real-world waste streams remain largely unexplored. This study presents the first comprehensive evaluation of emerging PFAS-selective materials across five distinct and challenging waste matrices (e.g., nanofiltration retentates and wet scrubber wastewaters), providing critical insights into their practical applicability. Overall, the PFAS-selective adsorbents exhibited faster adsorption kinetics and higher PFAS removal efficiencies in these complex matrices. The key to this enhanced performance is designing the interplay of multiple factors – including electrostatic attraction and hydrophobic capture, as well as pore configuration or fluorophilic interactions – that lead to higher affinity for PFAS removal. Mechanistic desorption studies demonstrated that a solvent-salt combination significantly improves PFAS recovery rates, up to 225-fold higher than single-component regenerants. These findings suggest a pathway toward sustainable PFAS remediation, minimizing environmental impact by enabling adsorbent reuse. Overall, the study highlights the high potential of these novel adsorbents to enhance PFAS management in diverse aqueous environments. Future work should focus on refining adsorbent formulations and regeneration protocols to maximize their practical application and adaptability to regulatory frameworks and environmental contexts.

1. Introduction

The treatment of per- and poly-fluoroalkyl substances (PFAS) in contaminated water sources is a global environmental priority due to their persistence, bioaccumulative nature, and connection to adverse health effects. Traditional treatment technologies often fall short of achieving the necessary low PFAS concentrations, particularly at ng L^{-1}

(ppt) to μg L^{-1} (ppb) levels [1]. Additionally, complex streams with high concentrations of inorganic salts, organic matter, and heavy metals further complicate the treatment process, making satisfactory PFAS removal difficult. Hard-to-treat streams include residual waste from nanofiltration (NF) or reverse osmosis (RO) retentates, landfill leachate, industrial processes, and wet scrubber wastewater, which often contain elevated PFAS concentrations. Exploring and developing treatment

options for these diverse matrices is crucial to providing practical performance expectations. Effective and sustainable solutions are urgently needed to manage these challenges and minimize PFAS release to the environment, thereby controlling PFAS at the source.

Residual waste streams can be classified as by-product streams resulting from water or wastewater treatment systems or other pollution control processes [2,3]. In this study, two major residual streams have been investigated. First is the waste stream (known as retentate, concentrate, or reject water) produced from municipal RO or NF water treatment systems. While RO and NF can effectively remove PFAS from diverse matrices to satisfy high water quality requirements, the retentate stream typically accounts for up to 20 % of the influent volume and concentrates PFAS and other undesired background constituents (i.e., dissolved salts, organics, trace metals, bacteria) [4]. Currently, retentates from full-scale treatment, which can contain hundreds of parts per trillion of total PFAS, [5,6] are disposed of by sanitary sewer, land application, or direct discharge to surface water [7]. The second residual stream is scrubber blowdown, where the wastewater quality depends on the original process. In this study, we include scrubber wastewaters resulting from two processes: 1) biosolids incineration at wastewater treatment plants and 2) thermal regeneration of spent activated carbon used at drinking water treatment plants. Although wet scrubber systems are designed to reduce gaseous emissions (e.g., heavy metals, particulate matter, CO_2, SO_x, NO_x, NH_3), PFAS have been detected in these residual streams at concentrations over 100 parts per trillion [8–12]. Since most facilities return scrubber water to the head of the treatment plant, polishing the residual stream prior to this return would minimize the PFAS load entering the system.

Adsorption, a simple physical–chemical process widely used for full-scale water treatment, has been identified as a viable and developed technology for removing PFAS from residual streams [13]. However, current sorbents like granular activated carbon (GAC) and ion exchange (IX) resins have significant limitations for removing PFAS from water. Their adsorption kinetics with PFAS are relatively slow, resulting in incomplete removal, especially at short contact times. Moreover, GAC and IX resins have low binding affinity for short-chain PFAS compared to long-chain compounds [14–17]. Another major challenge is the low PFAS concentrations, typically 4–7 orders of magnitude lower relative to background organic matter and ionic solutes. Interactions from competing constituents restrict PFAS access to available binding sites on GAC or IX resins. Consequently, complex water matrices can limit PFAS removal [18–21]. Despite the growing body of research on PFAS-selective adsorbents, their performance in concentrated waste streams with multiple competing constituents remains poorly understood. Previous studies have primarily focused on idealized conditions or simulated matrices, leaving a critical knowledge gap regarding real-world applicability.

Herein, we report a side-by-side comparison of five promising adsorbents for removing PFAS from complex residual waste streams. The adsorbents tested include three cyclodextrin-based polymers, one hydrogel, and a polymer-metal oxide hybrid. While previous studies have demonstrated PFAS removal in ideal or simple matrices [22,23], real adsorbent performance under interfering conditions in concentrated brines from NF and wastewater from wet scrubbers remains largely unstudied. This study directly addresses this knowledge gap. To advance sustainable PFAS remediation, selective adsorbents must demonstrate high affinity and resilience in real, interference-laden matrices. This is particularly critical for concentrated waste streams generated by PFAS removal technologies (e.g., filtration, foam fractionation) and landfill leachates, where treatment efficacy remains uncertain. We systematically examined PFAS removal across two NF concentrates (from groundwater and surface water treatment) and three wet scrubber effluents (from biosolids incineration and GAC regeneration). Adsorbent batch screening first prioritized rapid adsorption kinetics, and subsequent isotherm tests probed the high affinity and uptake capacity of top candidates under process-relevant conditions.

The results of this study provide critical insight to how PFAS-selective adsorption can be maintained in increasingly complex water qualities, which is essential to achieving wholistic PFAS management. Lastly, we explored regeneration of PFAS-selective adsorbents using solvent-salt combinations to enable adsorbent reuse. This comprehensive evaluation, which also tested GAC and IX resin in parallel for direct benchmarking, fills an important knowledge gap on the suitability and limits of these adsorbents for treating complex PFAS waste streams.

2. Materials and methods

2.1. Chemicals and reagents

Five PFAS were selected for the kinetics experiments in this study (PFNA, PFOA, PFHxS, PFBS, and HFPO-DA) to represent a set of carboxylic, sulfonic, short-chain, and long-chain PFAS (Section S4 in SI). PFAS stock solutions containing all five analytes were prepared at parts per million concentrations (ppm, mg L^{-1}) in methanol (Fisher, LCMS grade) using a volumetric flask. Isotherm experiments narrowed to PFOA and HFPO-DA, which represent two carboxylic PFAS with distinct properties (e.g., sorption affinities). Ultrapure Milli-Q (nanopure) water with 18.2 Ω-cm quality and 2 ppb total organic carbon (TOC) was used in all experimental solutions. Details regarding the reagents used in this study are provided in **Section S1**.

2.2. Targeted adsorbents

Five PFAS-selective adsorbents (**S1**, **S2**, **S3**, **H**, **A**) and two conventional adsorbents (**GAC**, **IX**) (Fig. 1 and Table S2) were evaluated for their PFAS removal performance in residual streams. Three distinct cyclodextrin-based polymers (CDPs), namely StyDex-1 (**S1**), StyDex-2 (**S2**), and StyDex-3 (**S3**), were obtained from the Dichtel Group at Northwestern University[24,25]. Previously, StyDex adsorbents have achieved near-complete removal for a wide range of PFAS at low concentrations,[24] but this study evaluates PFAS-selectivity in complex and real matrices. The hydrogel (**H**), designed with amine-functionalized perfluoropolyether crosslinkers, was obtained from the Leibfarth Group at the University of North Carolina at Chapel Hill [26]. Finally, a polymer-metal oxide adsorbent (**A**) commercialized as PFAS-selective was obtained from the manufacturer. Additional details for **A** remain undisclosed upon the company's request. The GAC (Filtrasorb 400) was obtained from Calgon, USA and the IX resin (PFA649E) was obtained from Purolite, USA. Additional details on the adsorbents, including basic characterization, are provided in **Section S2**.

2.3. Targeted residual waste streams

We obtained residual streams from five different treatment facilities across the US, which represent various scenarios of background organic and inorganic loads (Fig. 1). Two residual streams were retentates from NF units treating groundwater (**RT1**) and surface water (**RT2**). The first wet scrubber effluent resulted from thermal regeneration of spent GAC used at a drinking water treatment plant (**SC1**). Two more residual streams were collected from wet scrubber effluents from biosolids incineration at municipal wastewater treatment plants (**SC2** and **SC3**). All residual stream samples were collected in HDPE sampling containers and transported in coolers packed with ice packs. All samples were stored at 4 °C upon receipt, until use. The collected residual water samples were prefiltered in bulk (1.0 μm filter) to remove suspended solids and transferred to cleaned HDPE containers.

2.4. Analytical methods

Section S3 provides complete analytical details for water quality characterization and targeted PFAS analysis using liquid
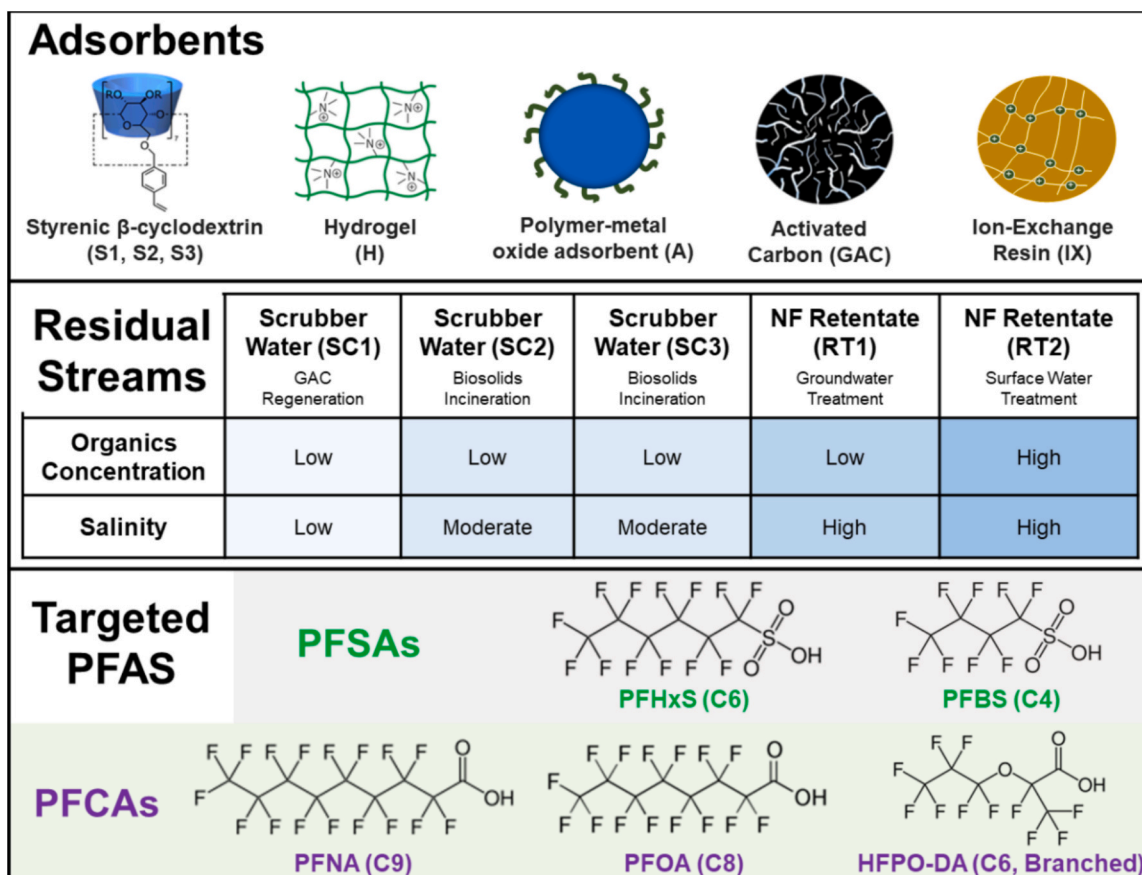
Fig. 1. Overview of the adsorbents, residual streams, and targeted PFAS investigated herein. Acronyms for adsorbents and residual streams are provided in parentheses.

chromatography with tandem mass spectrometry (LC-MS/MS). General water chemistry parameters were measured for all filtered residual stream samples, including volatile organic compounds (VOCs), polycyclic aromatic hydrocarbons (PAHs), chemical oxygen demand (COD), pH, conductivity, total organic carbon (TOC), specific UV absorbance (SUVA), primary anions (Cl⁻, NO_3^-, SO_4^{2-}), and elemental metals. All parameters were measured using standard methods.

To satisfy data quality and reporting, experimental samples were accompanied by quality assurance / quality control (QA/QC) samples. QA/QC requirements for targeted PFAS analysis are provided in Table S3. All data reported herein directly satisfied QA/QC requirements or were appropriately qualified. All QA/QC and experimental samples were stored under temperature-monitored refrigeration until analysis, except for when samples were prepared (e.g., extracted, diluted) for analysis. Sample preparation and LC-MS/MS method details for targeted PFAS analysis are detailed in Tables S4 and S3, respectively. Regardless of the analytical method, analysis occurred as soon as possible after sample preparation.

2.5. Kinetics and isotherm experiments

For batch adsorption kinetic experiments, the residual water samples were spiked with each of the five PFAS to provide an initial concentration of 10 μg L⁻¹ for retentate waters and 0.5 μg L⁻¹ for scrubber waters (pH 6 ± 1), which provided environmentally relevant concentrations for both types of residual streams [5,6,8,10,27]. For batch isotherm experiments, the nanopure and residual water samples were spiked with PFOA or HFPO-DA at initial concentrations ranging from 1 – 160 mg L⁻¹ This mg L⁻¹ range was selected in effort to parse adsorption selectivity between PFAS and matrix constituents and has been used for isotherm

experiments in ideal matrices. Adsorbent dose was 80 mg L⁻¹ for kinetics and 100 mg L⁻¹ for isotherm experiments. Kinetics and isotherm experiments were also conducted in nanopure water to determine benchmark performance. All batch experiments were carried out at room temperature in 125 mL HPDE bottles (kinetics) or 50 mL polypropylene centrifuge tubes (isotherm) on an orbital shaker at 200 rpm (Brunswick G10 Gyrotory Shaker).

Sampling points for kinetics experiments occurred at 0, 0.25, 0.50, 1, 4, 8, 12, and 24 h and for isotherm experiments at 24 h, where the bottles or tubes were sacrificed at each predetermined time point. These time points were selected to target the novel adsorbents, as conventional adsorbents – including GAC and IX – can require more than 24 h to reach equilibrium [28]. Adsorption was stopped at the desired time point by filtering the adsorbent-matrix sample through a 0.2 μm syringe filter (Pall Acrodisc; Whatman Puradisc) into a 15 mL centrifuge tube (Falcon, Fisher Scientific). The pseudo-second-order (PSO) model was applied empirically to compare batch kinetics results. For isotherm experiments in the control and residual streams, we report the distribution coefficient (K_d), which measures adsorption efficiency under more realistic and environmentally relevant conditions. Independent batch experiments were conducted in duplicate or triplicate for each adsorbent-matrix combination at all sampling points. Additional details on the kinetics and isotherm analysis are found in **Section S4**.

2.6. Desorption experiments

Three of the novel adsorbents (S1, H, A) were tested to explore PFAS desorption using three different regeneration solutions: 1) 400 mM ammonium acetate, 2) 50 % v/v methanol, and 3) 400 mM ammonium acetate in 50 % v/v methanol. The PFAS solution contained each of the

five analytes at an initial concentration of 100 ppb, µg L^{-1}. The adsorption period (1.5 h) in the PFAS solution was followed by an abbreviated regeneration period (4 h) in the regeneration solvent (50 mL). All adsorbent used in the adsorption cycle was used for the desorption cycle, minus losses during container transfer that are included in the reported values. In effort to minimize variability from mass losses, adsorbent dose was adjusted to 2 g L^{-1}. After each period, samples were centrifuged, and 5 mL supernatant was collected for LC-MS/MS analysis. As further detailed in Section S4, the adsorption–desorption procedure was repeated for up to three cycles.

3. Results and Discussion

3.1. Characterization of residual waste streams

Complex water matrices can inhibit PFAS adsorption due to adsorbent characteristics and competition for sorption sites [19,20,29,30]. Conventional adsorbents like GAC and IX resins show reduced adsorption capacity and kinetics for anionic PFAS due to sorption competition from organic matter [22,31–33]. Monovalent and divalent anions (e.g., Cl$^-$, NO$_3^-$, SO$_4^{2-}$) also hinder electrostatic interactions between anionic PFAS and the adsorbent surface, further decreasing sorption efficiency [30]. Evaluating novel adsorbents under these conditions in realistic scenarios is critical to identifying resilient options. This study includes residual streams with varying organic content and relevant anions, as summarized in Fig. 2, to comprehensively assess newly developed adsorbents. Detailed results from residual stream characterization are provided in Tables S5 and S6.

Scrubber Waters. Scrubber water quality data from water and wastewater treatment plants is limited. This study characterizes the water quality of three distinct scrubber waters, revealing the influence

Fig. 2. Concentrations for (a) dissolved organic carbon (DOC) and total dissolved solids (TDS) and (b) select inorganic constituents (Cl$^-$, NO$_3^-$, SO$_4^{2-}$, Ca) in the residual streams.

of process source on residual stream characteristics. SC1, from a GAC regeneration system, operates at lower temperatures compared to SC2 and SC3, which are from biosolids incinerators. Thus, SC2 and SC3, displayed similar key parameters, unlike SC1. For instance, DOC concentrations in SC2 and SC3 were four times higher than in SC1 (8.8 ± 0.1 and 9.4 ± 1.3 mg-C L^{-1} vs. 2.1 ± 0.9 mg-C L^{-1}), attributed to the high organic content of their influent. UV absorbance (SUVA$_{254}$) and conductivity followed the same trend, with SC2 and SC3 showing three times higher conductivity than SC1 (1235 and 1535 µS cm^{-1} vs. 417 µS cm^{-1}). SC1 had the lowest concentrations of nearly all 29 analyzed elements, including Ca, Mg, K, S, and Si (Table S5).

Operating temperature also affects VOC profiles. Lower temperatures in the SC1 system (370–925 °C; multiple hearth furnace) than those in the SC2 (425–925 °C; multiple hearth furnace) and SC3 (750–925 °C; fluidized bed) systems likely result in a higher diversity and abundance of VOCs, as less thermal energy limits the breakdown of complex organics. Each scrubber water displayed a distinct VOC profile, differing in the number of VOCs, relative abundance, and halogenated groups (Table S6). Chlorinated VOCs were largely undetected (≤2%), while fluorinated VOC content varied. SC1 contained 41 % fluorinated compounds, primarily methyl fluoride (CH$_3$F), also found in SC2 (12 %) and SC3 (3 %). Common non-fluorinated VOCs in SC2 and SC3 included dimethyl ether and 4-(1,1-dimethylpropyl) phenol. This temperature-dependent behavior highlights the importance of operational conditions in scrubber water quality evaluation.

NF Retentates. The source water significantly impacts the water quality of NF retentates. The retentates provided distinctly different DOC and COD values, where RT1 was characterized by low organics and high salinity and RT2 by high organics and high salinity (Table S5). DOC concentration in RT2, produced from a system receiving surface water, was ten times greater than RT1, produced from a system receiving groundwater. Moreover, COD in RT2 was over 35 times greater than RT1 (215 and 6 mg L^{-1}, respectively). RT2 provided a complex environment due to high organic accumulation (high DOC and COD). Conductivity was more similar than organic content, but RT1 and RT2 had unique inorganic ion and elemental compositions. RT2 had higher concentrations for all major anions (Cl$^-$, NO$_3^-$, and SO$_4^{2-}$) and sodium (Na), which supports its higher conductivity, whereas RT1 had higher concentrations for almost all elements (including Ca and Mg). Compared to municipal NF retentate water quality summarized elsewhere [34], RT1 and RT2 concentrations are low for Cl$^-$ and SO$_4^{2-}$ and high for NO$_3^-$ and Mg. The most abundant VOCs detected in both RT1 and RT2 are provided in Table S6. Non-fluorinated VOCs commonly found in RT1 and RT2 included dimethyl ether and cyclosiloxanes. Relative to RT1, RT2 showed much higher abundances of chlorinated and fluorinated VOCs at 24 % and 32 %, respectively.

3.2. Adsorption kinetics

Kinetics experiments in ultrapure water spiked with five PFAS revealed that several novel adsorbents (S1, S2, S3, H, P) had faster and higher PFAS removal than traditional adsorbents (IX, GAC) within the 24 h period (Fig. S1). The pseudo-second-order (PSO) rate constants (k_{obs}) by adsorbent for each adsorbent in ultrapure water are provided in Fig. 3. The PSO model was applied as a method for comparison; therefore, physical or mechanistic interpretation of the empirical model would provide erroneous insight [35,36]. The rate constant for GAC was not included because only the 24-hour contact time was measured. Moreover, the conventional adsorbents may not reach equilibrium within the 24-hour period.[28]

While equilibrium adsorption capacity is an important material property, practical treatment systems prioritize rapid PFAS uptake within operationally relevant timeframes (typically < 24 h). The novel adsorbents demonstrated significantly faster removal kinetics compared to GAC and IX, achieving > 90 % PFAS removal within 1 h, whereas conventional adsorbents often require multiple days to equilibrate. This
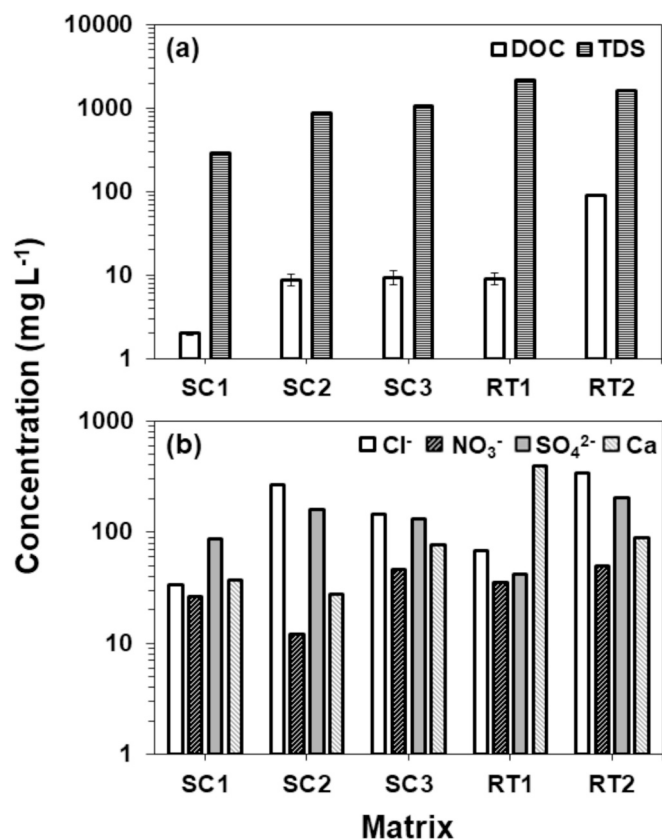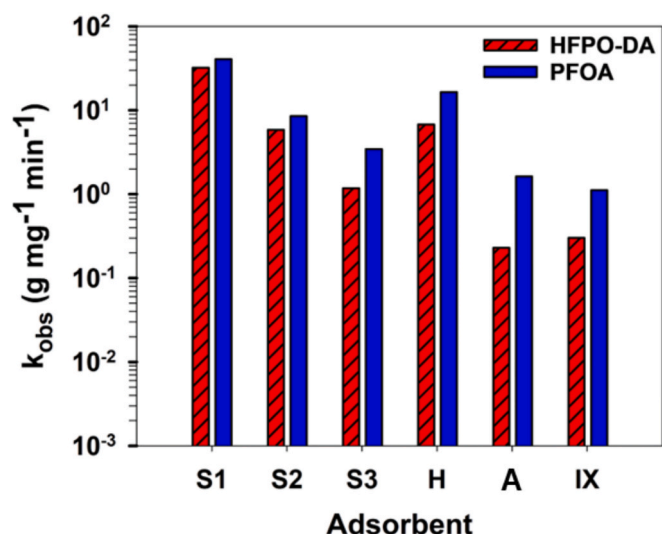
Fig. 3. The pseudo-second-order rate constant (k_{obs}) by adsorbent for HFPO-DA and PFOA in the control matrix (i.e., ultrapure water) spiked with all five analytes for an initial concentration of 500 ppt each. Adsorbent dose: 80 mg L^{-1}; pH 6 $\pm$ 1.

kinetic advantage is critical for real-world applications where hydraulic constraints limit contact time. The adsorption rate by adsorbent is as follows: S1 > H > S2 > S3 > A > IX. PFOA rate constants were higher or similar to HFPO-DA for all adsorbents. Cyclodextrin-based adsorbents (S1, S2, S3) rapidly adsorbed PFAS, with S1 achieving up to 2-fold greater than S2 and 10-fold greater than S3. S2 and S3 showed slower adsorption and less consistent removal than the other adsorbents for all five PFAS, leading to their exclusion from further experiments. Without S2 and S3, the remaining adsorbents removed at least 80 % of each analyte within 8 h. While conventional adsorbents (IX, GAC) closely matched the novel adsorbents (S1, H, A) after 24 h, S1, H, and A achieved over 90 % removal (100 ppt or less) in one hour or less.

Kinetics trends in the residual stream matrices (Figs. 4 and 5), which featured diverse water quality characteristics, largely mirrored those in the control matrix. However, adsorbent performance decreased with the introduction of matrix components, especially at early contact times.
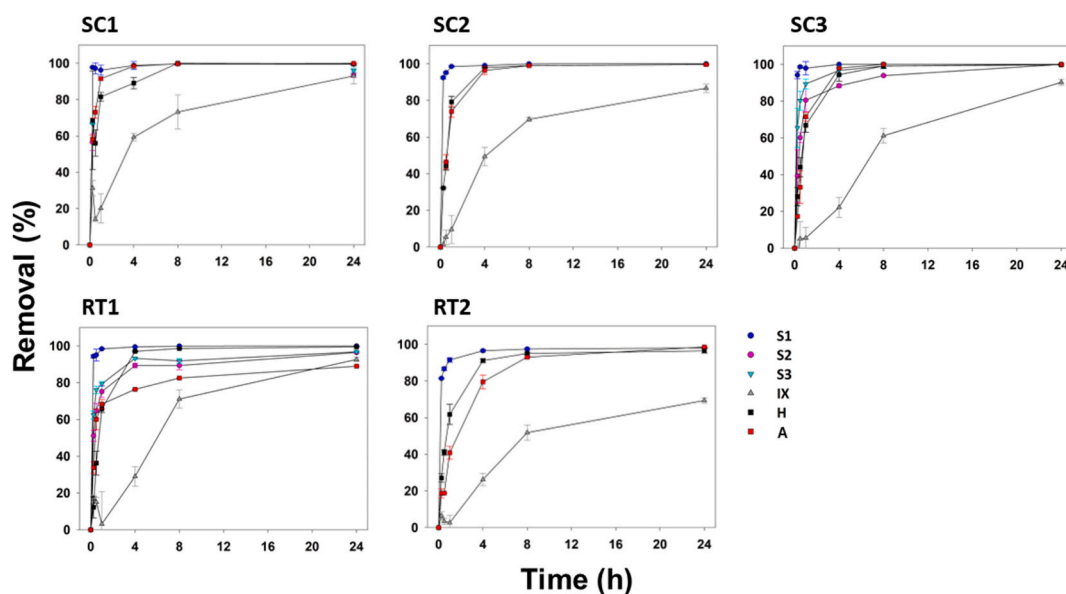
Among conventional adsorbents, IX outperformed GAC but exhibited slow kinetics relative to the novel adsorbents. IX may not reach equilibrium within the period tested herein. GAC had drastically lower removals in the residual matrices than in the control, removing only 48 % PFOA and 29 % HFPO-DA in SC1 (lowest salinity and organic content) after 24 h. In contrast, the novel adsorbents (S1, H, and A) removed over 99 % PFOA (< MRL at 10 ppt) and over 83 % HFPO-DA in SC1 after 24 h. For all adsorbents in each residual stream, HFPO-DA proved to be the most challenging analyte to remove quickly and completely.

Fig. 6 compares PFAS removal (%) by the novel adsorbents (S1, H, A) across the residual stream matrices at 0.5 and 8 h time points. Despite challenging conditions in the residual streams, S1 provided robust adsorption in the residual streams at 0.5 h, achieving the highest HFPO-DA removal at 78 % and over 95 % PFOA removal in all matrices. The most complex matrix (RT2) inhibited HFPO-DA removal by S1 and A at 0.5 h, but S1 still achieved over 85 % PFOA removal. Although S1 provided higher removals than H at the short contact time, H had the most robust and consistent performance across all matrices at the longer contact time with average removals of 99 $\pm$ 2 % PFOA and 87 $\pm$ 11 % HFPO-DA across all matrices. Adsorbent A removed PFOA and HFPO-DA to a similar extent in most matrices but was less effective than S1 and H.

The physical and chemical characteristics of the novel adsorbents support these kinetics trends. S1′s cationic amine attracts anionic carboxylic or sulfonic groups electrostatically, while its β-cyclodextrin cavity forms stable complexes with fluorocarbons [24,37,38]. The rapid adsorption demonstrated by S1 may also be encouraged by its tailored pore structure [24], where meso- and macropores can favorably maintain pore availability for PFAS adsorption [39]. These features enable S1′s rapid removal of both short-chain and long-chain PFAS compounds from complex matrices. Similarly, H promotes electrostatic interaction through its ammonium-functionalized perfluoropolyether crosslinkers, and fluorophilic interactions between PFAS and the fluorinated crosslinker enhance removal at longer contact times [23,26]. Although the structure of A remains unknown, its performance suggests that it follows similar general removal mechanisms as the other novel adsorbents. Overall, the novel adsorbents, particularly S1 and H, demonstrated exceptional performance in removing PFAS from complex water matrices due to intentional and customized structures.

Fig. 4. Removal (%) by adsorbent for PFOA in each matrix over the 24 h kinetics period. Matrix spiked with all five analytes. Scrubber (SC) initial PFAS concentration: 500 ppt each. Retentate (RT) initial PFAS concentration: 10 ppb each. Adsorbent dose: 80 mg L^{-1}; pH 5–7.
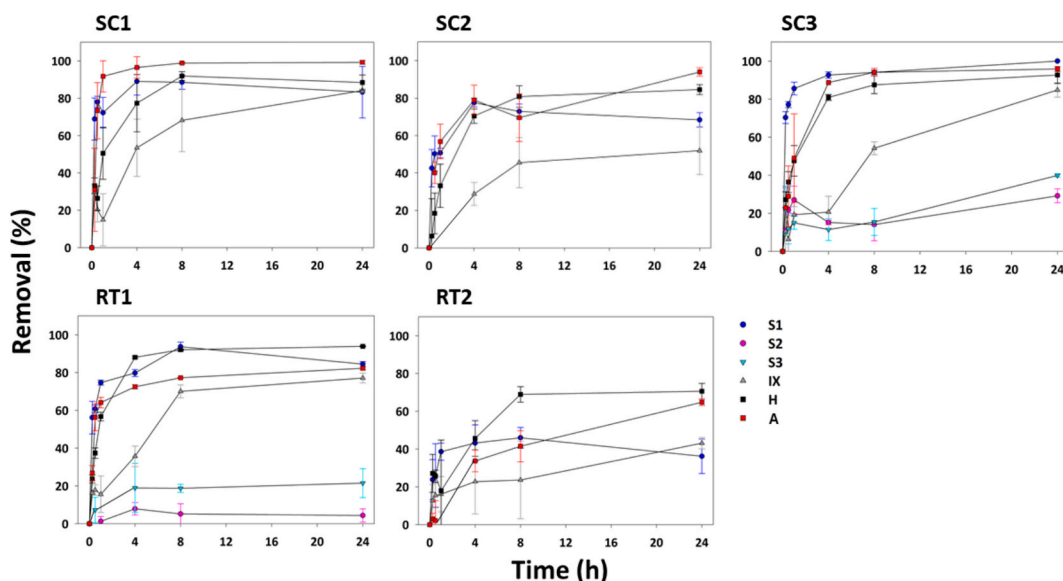
Fig. 5. Removal (%) by adsorbent for HFPO-DA in each matrix over the 24 h kinetics period. Matrix spiked with all five analytes. Scrubber (SC) initial PFAS concentration: 500 ppt each. Retentate (RT) initial PFAS concentration: 10 ppb each. Adsorbent dose: 80 mg L^{-1}; pH 5–7.
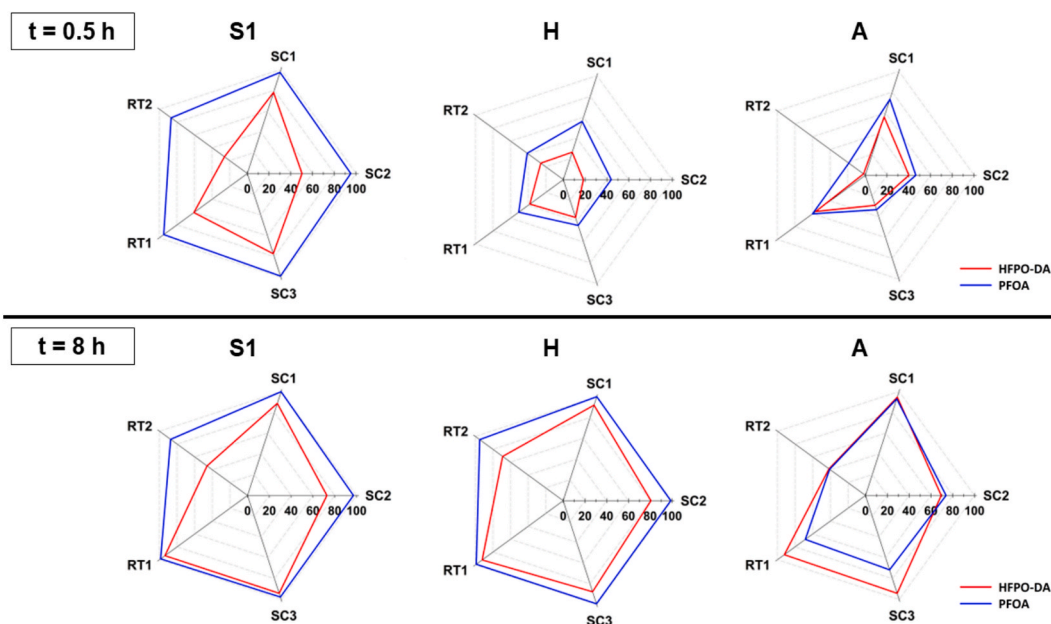

Fig. 6. PFOA and HFPO-DA removal (%) by the novel adsorbents S1, H, and A in the residual stream matrices at 0.5 h (top) and 8 h (bottom) contact time. Matrix complexity (salinity, organics) increases clockwise from SC 1 (least complex) to RT 2 (most complex). Scrubber (SC) initial PFAS concentration: 500 ppt each. Retentate (RT) initial PFAS concentration: 10 ppb each. Adsorbent dose: 80 mg L-1; pH 6 ± 1.

3.3. Adsorption isotherm

Adsorption isotherms of PFOA and HFPO-DA in the control matrix (i. e., ultrapure water) reveal different capacities (Q_e) for the high-performing adsorbents (S1, H, and A) (Fig. 7). Full adsorption isotherms for all adsorbents are provided in the SI (Fig. S2). Although GAC and IX may ultimately reach higher equilibrium capacities over extended contact periods, this study focuses on adsorption performance under timeframes relevant to engineered treatment systems. The observed differences in PFAS uptake kinetics highlight the advantage of these novel adsorbents for applications requiring high removal efficiencies in short durations. H demonstrated the highest capacity for GenX (655 ± 20 mg g^{-1}), which was over two times greater than the maximum capacity with S1 (275 ± 40 mg g^{-1}). However, both S1 and H

favored PFOA adsorption, approaching capacities of 900 mg g^{-1}. Compared with β-cyclodextrin capacities reported elsewhere under the same conditions, [40] S1 provided comparable HFPO-DA and higher PFOA capacities. In contrast to S1 and H, which had higher capacities for PFOA, A had similar capacities for both compounds (near 600 mg g^{-1}). IX did not provide higher capacities than the novel adsorbents, but it did follow a similar behavior as H, such that its capacity for PFOA was 1.75-fold greater than for HFPO-DA. Although IX may not have reached equilibrium within the 24 h period, IX and H exhibited similar behaviors to support their similar adsorption mechanisms.

Our approach in using complex residual streams contrasts with previous work, where PFAS adsorption is most typically evaluated in simulated or ideal matrices (e.g., ultrapure or deionized water) [20,27,41]. Traditional adsorption models such as Langmuir and
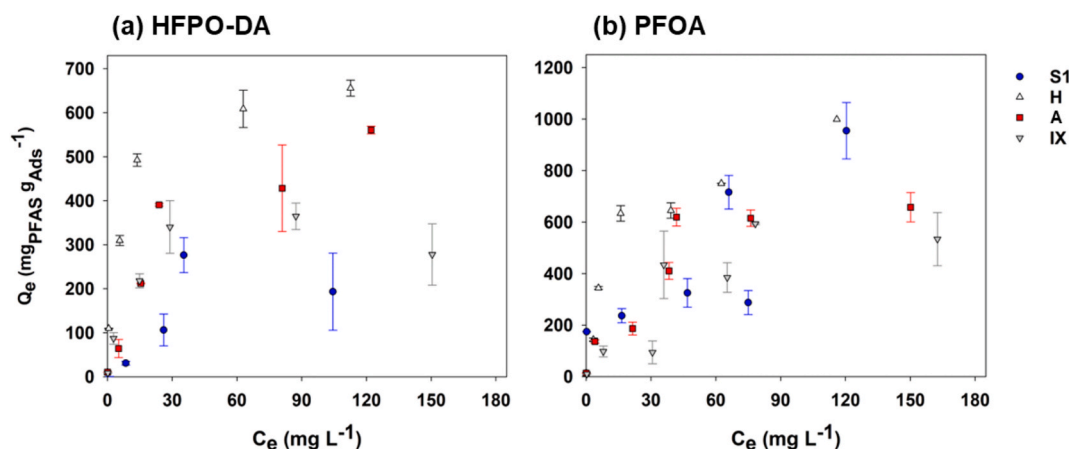
Fig. 7. Adsorption isotherm of (a) HFPO-DA and (b) PFOA on the adsorbents S1, H, A, and IX in the control matrix. Error bars represent standard deviation from replicate experiments. Initial PFAS concentration: 1–160 mg L^{-1}; contact time: 24 h. Adsorbent dose: 100 mg L^{-1}; pH 6 $\pm$ 1.

Freundlich assume a single-solute system with homogeneous adsorption sites, making them unsuitable for complex environmental matrices with multiple competing constituents. In contrast, the distribution coefficient (K_d) approach was used here, as it allows direct comparison of adsorption efficiency across diverse wastewater matrices with varying ionic strength and organic content. Competitive adsorption trends between different PFAS species and matrix constituents provide additional mechanistic insights, revealing the role of electrostatic interactions and hydrophobic capture in complex conditions (Fig. 8 **and S3**). K_d (L kg^{-1}) was calculated using Equations (1) and (2) below:

$$q_e = \frac{C_0 - C_e}{m_{ads}} * V \tag{1}$$

$$K_d = \frac{q_e}{C_e} \tag{2}$$

where q_e is the equilibrium adsorption density (μg kg^{-1}), C_0 is the initial PFAS concentration (μg L^{-1}), C_e is the PFAS concentration at equilibrium (μg L^{-1}), m_{ads} is the mass of adsorbent used (kg), and V is the solution volume (L). K_d values were calculated at equilibrium concentrations (C_e = 10–20 mg L^{-1}) far from adsorbent saturation (q_m), and the corresponding K_d values measure adsorption efficiency under more realistic and environmentally relevant conditions. Moreover, K_d values can be used to compare relative adsorbent performance.[42] Tables S7 and S8 reports the average C_e and log transformed K_d for the adsorbents in each matrix. Variation in Q_e was anticipated due to the high dilution factor required for targeted PFAS analysis; this dilution level was necessary to avoid instrument saturation and to satisfy LC-MS/MS sensitivity constraints ($\leq$ 20,000 ppt per analyte). Additionally, unlike typical isotherm studies that draw multiple aliquots from a single experimental batch, this study conducted independent batch experiments for each
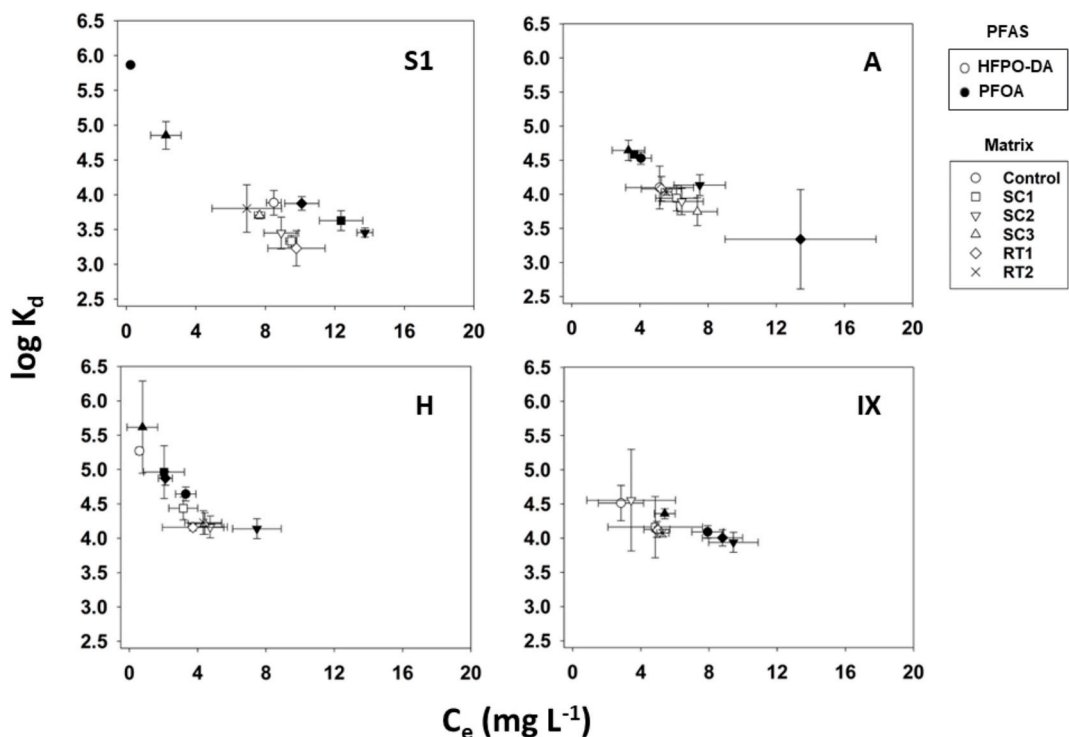

Fig. 8. Average log transformed distribution coefficients (log K_d) of HFPO-DA ($\circ$ unfilled) and PFOA ($\bullet$ filled) on S1, H, A, and IX by matrix (symbols). Error bars represent standard deviation from replicate experiments. Error bars that are not visible are smaller than the symbol scale. Adsorbent dose: 100 mg L^{-1}; pH 6 $\pm$ 1.

data point, meaning that minor variations in matrix composition, competing ions, and organic content could contribute to observed fluctuations. Despite these variations, the overall adsorption trend remains consistent, supporting the reliability of the data.

Overall, HFPO-DA removal was more consistent across the residual matrices than PFOA removal. Moreover, the adsorbents with the greatest capacity and affinity for PFOA were not the same adsorbents as for HFPO-DA. Across the matrices, S1 largely provided better PFOA removal than A and IX, but A and IX provided better HFPO-DA removal. However, H provided the greatest affinity and capacity for both PFOA and HFPO-DA across a wide concentration range in the diverse residual streams. This trend reinforces the impact of tailored adsorbent properties on resulting adsorbent-adsorbate interactions. Notably, IX contends with the novel adsorbents at lower concentrations (comparable log K_d, Fig. 8) but has limited capacity at higher concentrations (lower Q_e, Fig. 7) as it may not have reached equilibrium under these conditions. Adsorbent A provided consistent HPFO-DA removal but affinity and capacity for PFOA varied. PFOA adsorption on S1 and HFPO-DA adsorption on H were exceptional when matrix complexities were absent, reaching a clear maximum in the control matrix.

The distinct kinetics and equilibrium behavior of the adsorbents reviewed here reinforce the critical role of adsorbent properties on adsorption performance in complex matrices. While ion exchange materials often have lower BET surface areas, both H and IX are equipped with a positive functional group to promote adsorption through electrostatic interactions. In addition to electrostatic interactions, H further benefits from fluorous interactions between the fluorinated PFAS and its fluorinated crosslinkers and end groups.[23,26] These results support the hypothesis that fluorine–fluorine interactions provide PFAS selectivity even in the presence of competing components [43]. S1 also contains a positive functional group for electrostatic interactions, but cyclodextrin-based adsorbents also rely on hydrophobic interactions with the interior cavity that is formed by the cylic glucose monomers ("guest–host" interactions) [24,44,45]. Relative to H, S1 may have more limited capacity in complex matrices due to competing guest–host pairings. Future work should focus on evaluating existing multicomponent adsorption and ion-exchange models for PFAS removal in complex matrices. However, for real-world treatment applications, the K_d approach provides the most practical and environmentally relevant metric for comparing PFAS adsorption efficiency across diverse wastewater streams.

3.4. Effects of inorganic ions and organics constituents

The complex water quality of the residual streams provided insight into the unique PFAS adsorption behavior of both conventional and novel adsorbents. The cyclodextrin-based adsorbents (S1, S2, and S3) demonstrated varied PFAS adsorption in the control and the residual matrices. The unique PFAS adsorption trends observed for each cyclodextrin adsorbent are reinforced elsewhere, where neutral cyclodextrin favors zwitterionic PFAS, and cationic cyclodextrin provides robust PFAS adsorption [46,47]. Here, S1 is the only cyclodextrin adsorbent with cationic functionalization, which provided faster removal than S2 and S3 (no charge) in all matrices. The superior performance of S1 is most notable with HFPO-DA, where S1 maintains high removal across all matrices after 8 h (82 ± 20 % removal). A recent study has compared two cationic functionalized cyclodextrins (quaternary ammonium or phosphonium) and found that both responded similarly to the addition of organics (i.e., humic acid, HA) and various salts, where PFAS adsorption was most negatively impacted by SO_4^{2-}.[21] Similarly, S1 had the most inhibited adsorption for HFPO-DA in the two matrices with the highest total inorganic anion concentrations: RT2 and SC2.

For conventional adsorbents, calcium (Ca^{2+}) has also been shown to interrupt the adsorption interactions for activated carbon (AC) (direct site competition) and anion exchange resin via chemical complexation [21]. In contrast, enhanced adsorption for HFPO-DA and short-chain

PFAAs on AC and IX can occur in the presence of organics or inorganic cations [21]. The distinct responses of different adsorbents to matrix cations highlight their unique removal mechanisms. Adsorbent A exhibited reduced PFOA capacity in RT1, which had the highest Ca2+ concentration (390 mg/L), suggesting cation bridging effects or charge screening altered surface interactions, reducing PFAS affinity. In contrast, H and IX maintained consistent performance due to their ion-exchange-driven mechanisms, which interact directly with anionic PFAS, making them less susceptible to cation interference. While Ca2+ has been shown to enhance PFAS adsorption on metal-grafted GAC via surface complexation, A's distinct chemistry likely results in different interactions. S1 also showed reduced performance in SC1, SC2, and RT1, but this was primarily due to competing anions (e.g., sulfate) rather than cationic effects, consistent with findings on cyclodextrin-based materials. These differences emphasize how functional group chemistry dictates adsorbent resilience to specific matrix components [21].

IX provided the fastest HFPO-DA adsorption (% removal), excluding the control matrix, in the least complex scrubber water (SC1) and the retentate with moderate organics and high salinity (RT1). IX maintained HFPO-DA adsorption in RT1, likely due to the increased salinity (2160 mg L^{-1} TDS) and potential salting out of the PFAS molecules that promoted their interaction with the resin. IX has also exhibited enhanced PFAS adsorption in the presence of simulated organic content (i.e., humic acid, HA) at low concentrations (1 mg L^{-1}) [21]. Relative to the control matrix, IX did not demonstrate improved adsorption (capacity or kinetics) in the low organic matrix (SC1, 2 mg L^{-1}) or in the remaining residual matrices (8–90 mg L^{-1} DOC)

Relative to IX, H provided higher K_d for PFOA and faster kinetics for HFPO-DA. Moreover, H had high and robust performance across the matrices, which supported the introduction of fluorophilic interactions through its fluorinated crosslinkers and end groups. The presence of fluorinated organic co-contaminants in wastewater can hinder PFAS adsorption due to competitive fluorophilic interactions. Prior studies have shown that multiple fluorinated species can compete for sorption sites, reducing removal efficiency. This competition is influenced by the degree of fluorination, molecular structure, and spatial arrangement of fluorine atoms, with highly fluorinated organics forming stronger fluorophilic interactions [48]. Additionally, co-contaminants with hydrophobic backbones can obstruct PFAS access to binding sites, further decreasing adsorption efficiency [49]. These mechanisms explain why adsorbent H exhibited lower PFOA removal in matrices with elevated fluorinated VOC content, aligning with prior findings on competitive fluorophilic interactions [50]. Understanding these interactions is crucial for optimizing adsorbent design in real-world wastewater treatment applications.

With H, the lowest K_d for PFOA was achieved in SC2, which had the second highest fraction of fluorinated VOCs (26 %). In contrast, the highest K_d was achieved in SC3, which had similar organic loading, salinity, and inorganic composition but the lowest fraction of fluorinated VOCs (3 %). Unlike its varied capacity for PFOA, H maintained consistent HFPO-DA removal despite varied water quality; this suggests that the fluorophilic interactions may be less important for removing PFECA and other short-chain PFAS in complex matrices. The limited impact of fluorophilic interactions with HFPO-DA is further supported when HFPO-DA adsorption on H is compared to that on IX (ion exchange, hydrophobic interactions only). H and IX have nearly identical average log K_d values from all the residual matrices (4.24 ± 0.11 and 4.21 ± 0.20, respectively), which suggests that HFPO-DA adsorption on H relies primarily on ion exchange and hydrophobic interactions.

Adsorbent A adsorption capacity for HFPO-DA was nearly unchanged across all matrices, including the control matrix. While PFOA capacity was also similar across matrices, A capacity for PFOA dropped drastically in RT1 (from 4.53 in the control to 3.34 in RT1). RT1 provides an insightful composition to matrix interferences with A because it has the highest total cation concentration (682 mg L^{-1}), with Ca^{2+} contributing over 57 % of the total cation content on a mass basis (390

mg L^{-1}). This may suggest that high cation concentrations, primarily Ca^{2+}, can drastically interfere with long-chain PFCA adsorption on A. Lastly, PFAS chemical properties, including hydrophobicity and molar volume (steric interactions), have shown positive correlations with K$_d$ on activated carbons and cyclodextrin adsorbents [42]. The K$_d$ values for the cyclodextrin (S1) presented herein agree with this correlation, where PFOA (C-8) had higher values than HFPO-DA (C-6). The polymer-metal oxide adsorbent (A) also agrees, except for the complex retentate matrix. Moreover, the data also reflect the effects of molecular structure – including the functional group, non-fluorinated carbons and adjacently bonded atoms, and charge state – on PFAS adsorption [42]. As a whole, the median K$_d$ for oxygen-containing HFPO-DA was lower than that for linear PFOA across the same matrices (log K$_d$ = 4.10 and 4.39, respectively). This supports experimental and theoretical adsorption trends investigated elsewhere [42,51]. For diverse adsorbents (carbon, cyclodextrin, resin, inorganic), lower K$_d$ values were obtained for PFSAs containing oxygen in the backbone relative to linear PFSAs [42]. Further, PFOA has been estimated to have more favorable (spontaneous) interactions (Van Der Waals, hydrogen bonding) with activated carbon than HFPO-DA (GenX) [51]. However, IX and H deviated from this overall trend in several matrices, where K$_d$ was greater for HFPO-DA than PFOA, which may suggest that equilibrium was not attained.

3.5. Desorption mechanisms

Control desorption experiments were conducted to demonstrate the regenerability of novel adsorbents and to further elucidate the adsorption/desorption mechanisms for PFAS removal. The three novel adsorbents (S1, H, A) demonstrated near-complete and consistent PFAS adsorption (1.5 h) after multiple adsorption–desorption cycles, supporting adsorbent reuse after exposure (4 h) to regeneration solutions. Despite near-complete adsorption after multiple cycles, total PFAS (ΣPFAS) recovery (desorption) varied by regeneration solution and adsorbent, as shown in Fig. 9. Among the tested regeneration solutions, combining an organic solvent with a basic salt (50 % v/v methanol with 400 mM ammonium acetate, MeOH + AA) was the most effective in recovering adsorbed PFAS for all three adsorbents. On average, ΣPFAS recovery using MeOH + AA was 35-fold greater than using ammonium acetate (AA) alone and 225-fold greater than using methanol (MeOH) alone. This enhanced recovery is attributed to the synergistic effect of the organic solvent and salt: the salt moderates electrostatic interactions at the head of the PFAS molecules, while the organic solvent disrupts hydrophobic interactions at the tail by reducing solution polarity and increasing solubility. This mechanism aligns with previous studies on

conventional resin regeneration, which reported similar interactions. [20,52].

However, despite the superior performance of MeOH + AA in achieving the highest ΣPFAS recovery, the desorption patterns for individual PFAS compounds remained consistent across all regeneration solutions. Recoveries by compound can be ranked as HFPO-DA > PFBS > PFOA > PFHxS, PFNA (Table S9). The recovery trend agrees with the results from adsorption kinetics and capacities, where HFPO-DA and PFBS are the most easily recovered adsorbates and most difficult to adsorb. The recovery trend also reflects adsorbate structure/properties. The long-chain, linear compounds (PFHxS, PFOA, PFNA) had lower recoveries that can be attributed to their higher hydrophobicity. The influence of adsorbate structure/properties is also observed between HFPO-DA and PFHxS. Despite the same carbon chain length (C-6), the branched HFPO-DA structure provided distinctly higher average recoveries than the linear PFHxS structure (over 10-fold greater in AA, 30-fold greater in MeOH + AA).

When comparing adsorbents, H provided the most consistent and highest average ΣPFAS recovery in MeOH + AA (~22 %) under the tested conditions (i.e., abbreviated desorption period, 4 h). S1 and A followed with average ΣPFAS recovery near 16 % and 15 %, respectively. While MeOH provided the lowest recoveries for all adsorbents, H in MeOH had 5 to 10-fold greater ΣPFAS recoveries than S1 and A. Moreover, H had the highest recovery for each compound, suggesting that the hydrophobic and fluorophilic interactions between H and the PFAS tail are most easily interrupted. The promising results from these findings reinforce the need to fully evaluate novel adsorbent regenerability using best practices [53,54]. Based on these observations, future studies on the regeneration of novel adsorbents should focus on optimizing regeneration parameters — such as the type of salt, choice of organic solvent, and specific adsorbent properties — to maximize ΣPFAS recovery. Understanding the interplay between adsorbate properties, solvent composition, and adsorbent characteristics will be critical in advancing PFAS remediation technologies.

4. Conclusions and environmental implications

The results of this study provide compelling evidence for the great potential of novel adsorbents in addressing the persistent challenge of PFAS contamination in complex waste streams. Conventional adsorbents such as GAC and IX resins have long been the standard in water treatment for the removal of organic and ionic contaminants. However, they exhibit certain limitations toward PFAS removal applications: relatively slow adsorption kinetics, poor selectivity for short-chain PFAS, and susceptibility to matrix interferences. The novel adsorbents evaluated here, which include cyclodextrin-based polymers, a hydrogel, and a polymer-metal oxide hybrid, offer a promising alternative solution. These materials demonstrated enhanced PFAS removal efficiency and the ability to function effectively under harsh environmental conditions that impede traditional sorbents. Crucially, the novel adsorbents showed a unique balance between adsorption capacity and kinetics, which is pivotal for real-world applications where rapid and complete PFAS removal is required. Cyclodextrin-based polymers, for instance, can leverage their macrocyclic, porous structures to enable highly specific guest–host interactions with PFAS molecules, leading to faster uptake and higher selectivity. The hydrogel, designed with amine-functionalized perfluoropolyether crosslinkers, offers another layer of selectivity by combining electrostatic attractions with fluorophilic interactions. The symbiotic contribution of multiple factors – including electrostatic attraction and hydrophobic capture, as well as pore configuration and fluorophilic interactions – captures a broader spectrum of PFAS compounds and maintains high performance even in matrices with high salinity and organic loads, where conventional adsorbents typically suffer.

The implications of these findings are far-reaching if implemented at scale to manage residual waste streams, such as those from
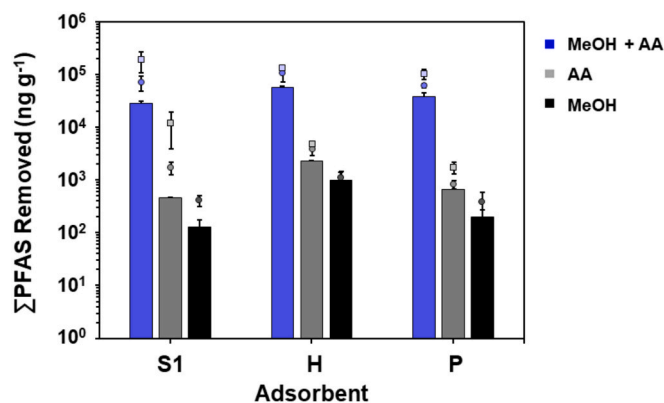

Fig. 9. Average total PFAS (ΣPFAS) removed from each adsorbent (S1, H, A) by regeneration solution (50 % v/v methanol, MeOH; 400 mM ammonium acetate, AA; MeOH + AA) during the first (bar), second (○ circle), and third (□ square) regeneration cycle. Cycle 3 was not collected for MeOH; therefore, the last cycle for MeOH is Cycle 2. Error bars represent standard deviation from replicate experiments. Error bars that are not visible are smaller than the symbol scale.

nanofiltration retentates and wet scrubber systems. These streams are challenging to treat due to their complex chemical compositions and high PFAS concentrations. Moreover, the regeneration of these materials using a mixed solvent-salt solution suggests a lower frequency of adsorbent replacement and reduced environmental footprint due to minimized waste generation. This could make advanced PFAS remediation economically viable even for smaller municipalities or facilities struggling with resource constraints. While this study provides a comparative evaluation of PFAS-selective adsorbents under batch conditions, future work will focus on flow-through column studies to assess breakthrough behavior, long-term capacity, and scalability for full-scale treatment applications.

However, the findings also raise critical questions about the scalability and optimization of these novel materials. While the solvent-salt regeneration approach was effective, it also presents practical challenges, such as managing solvent recovery and subsequent destruction of PFAS. Additionally, the variability in desorption efficiency among different PFAS types underscores the need for a more nuanced understanding of adsorbate-adsorbent interactions in flow-through systems. Future research must delve deeper into the molecular mechanisms that govern these interactions, as this knowledge could unlock an even better design of novel adsorbents. Tailoring regeneration protocols to the specific chemical nature of the PFAS being targeted (e.g., short-chain versus long-chain compounds or sulfonates versus carboxylates) could further enhance the efficacy and sustainability of these systems.

5. Disclaimer

The U.S. Environmental Protection Agency, through its Office of Research and Development, funded and managed, or partially funded and collaborated in, the research described herein. It has been subjected to the Agency's administrative review and has been approved for external publication. Any opinions expressed in this paper are those of the author(s) and do not necessarily reflect the views of the Agency. Therefore, no official endorsement should be inferred. Any mention of trade names or commercial products does not constitute endorsement or recommendation for use. I.M.H. and F.A.L. are inventors on a patent that cover the perfluoropolyether-based sorbents (US17/237,188). W.R.D. owns equity and/or stock options in Cyclopure, Inc. (Cyclopure), which is commercializing β-CD polymers for water treatment and other applications. W.R.D. has previously served as officers and/or advisors for Cyclopure. Cyclopure was not involved in the research described in this manuscript.

CRediT authorship contribution statement

Ashley Hesterberg Butzlaff: Writing – original draft, Methodology, Investigation, Formal analysis, Data curation. **Bineyam Mezgebe:** Investigation, Formal analysis. **Ashton Collins:** Investigation, Formal analysis. **Zhi-Wei Lin:** Writing – review & editing, Investigation, Formal analysis. **Dyandra Lassalle-Vega:** Formal analysis. **Irene M. Harmody:** Resources, Formal analysis. **Orlando Coronell:** Writing – review & editing, Validation, Resources. **Frank A. Leibfarth:** Writing – review & editing, Resources, Methodology. **William R. Dichtel:** Writing – review & editing, Resources, Methodology. **Mallikarjuna Nadagouda:** Writing – review & editing, Resources, Project administration. **Mohamed Ateia:** Writing – original draft, Validation, Supervision, Methodology, Funding acquisition, Conceptualization.

Declaration of competing interest

The authors declare that they have no known competing financial interests or personal relationships that could have appeared to influence the work reported in this paper.

Appendix A. Supplementary data

Supplementary data to this article can be found online at https://doi.org/10.1016/j.cej.2025.161983.

Data availability

Data will be made available on request.

References

[1] D. Ackerman Grunfeld, D. Gilbert, J. Hou, A.M. Jones, M.J. Lee, T.C.G. Kibbey, D. M. O'Carroll, Underestimated burden of per- and polyfluoroalkyl substances in global surface waters and groundwaters, Nature Geoscie 17 (4) (2024) 340–346, https://doi.org/10.1038/s41561-024-01402-8.

[2] Drinking Water Treatment Plant Residuals Management: Summary of Residuals Generation, Treatment, and Disposal at Large Community Water Systems., United States Environmental Protection Agency, EPA 820-R-11-003, 2011.

[3] Tech Brief: Water Treatment Plant Residuals Management, National Drinking Water Clearinghouse, 1998.

[4] H. Valdés, A. Saavedra, M. Flores, I. Vera-Puerto, H. Aviña, M. Belmonte, Reverse Osmosis Concentrate: Physicochemical Characteristics, Environmental Impact, and Technologies, Membranes (2021).

[5] V. Franke, P. McCleaf, K. Lindegren, L. Ahrens, Efficient removal of per- and polyfluoroalkyl substances (PFASs) in drinking water treatment: nanofiltration combined with active carbon or anion exchange, Environ. Sci. Water Res. Technol. 5 (11) (2019) 1836–1843, https://doi.org/10.1039/C9EW00286C.

[6] V. Franke, M. Ullberg, P. McCleaf, M. Wålinder, S.J. Köhler, L. Ahrens, The Price of Really Clean Water: Combining Nanofiltration with Granular Activated Carbon and Anion Exchange Resins for the Removal of Per- And Polyfluoralkyl Substances (PFASs) in Drinking Water Production, ACS ES&T Water 1 (4) (2021) 782–795, https://doi.org/10.1021/acsestwater.0c00141.

[7] C.C. Murray, A.S. Gorzalski, E.J. Rosenfeldt, C. Owen, C. Moody, Characterizing PFAS concentrations in drinking water treatment residuals, AWWA Water Sci. 6 (2) (2024) e1367.

[8] B.A. Seay, K. Dasu, I.C. MacGregor, M.P. Austin, R.T. Krile, A.J. Frank, G.A. Fenton, D.R. Heiss, R.J. Williamson, S. Buehler, Per- and polyfluoroalkyl substances fate and transport at a wastewater treatment plant with a collocated sewage sludge incinerator, Sci. Total Environ. 874 (2023) 162357, https://doi.org/10.1016/j.scitotenv.2023.162357.

[9] L.J. Winchell, J.J. Ross, M.J.M. Wells, X. Fonoll, J.W. Norton Jr, K.Y. Bell, Per- and polyfluoroalkyl substances thermal destruction at water resource recovery facilities: A state of the science review, Water Environ. Res 93 (6) (2021) 826–843, https://doi.org/10.1002/wer.1483.

[10] L.J. Winchell, M.J.M. Wells, J.J. Ross, F. Kakar, A. Teymouri, D.J. Gonzalez, K. Dangtran, S.M. Bessler, S. Carlson, X.F. Almansa, J.W. Norton Jr, K.Y. Bell, Fate of perfluoroalkyl and polyfluoroalkyl substances (PFAS) through two full-scale wastewater sludge incinerators, Water Environ. Res 96 (3) (2024) e11009, https://doi.org/10.1002/wer.11009.

[11] S. Björklund, E. Weidemann, S. Jansson, Emission of Per- and Polyfluoroalkyl Substances from a Waste-to-Energy Plant—Occurrence in Ashes, Treated Process Water, and First Observation in Flue Gas, Environmental Science & Technology 57 (27) (2023) 10089–10095, https://doi.org/10.1021/acs.est.2c08960.

[12] J. Strandberg, R. Awad, D.J. Bolinius, J.-J. Yang, J. Sandberg, M.A. Bello, L. Gobelius, L. Egelrud, E.-L. Härnwall, PFAS in waste residuals from Swedish incineration plants: A systematic investigation, IVL Swedish Environmental Institute, No. 2422, 2021.

[13] E.W. Tow, M.S. Ersan, S. Kum, T. Lee, T.F. Speth, C. Owen, C. Bellona, M. N. Nadagouda, A.M. Mikelonis, P. Westerhoff, C. Mysore, V.S. Frenkel, V. deSilva, W.S. Walker, A.K. Safulko, D.A. Ladner, Managing and treating per- and polyfluoroalkyl substances (PFAS) in membrane concentrates, AWWA Water Sci. 3 (5) (2021) e1233.

[14] Y. Zhang, A. Thomas, O. Apul, A.K. Venkatesan, Coexisting ions and long-chain per- and polyfluoroalkyl substances (PFAS) inhibit the adsorption of short-chain PFAS by granular activated carbon, J. Hazard. Mater. 460 (2023) 132378, https://doi.org/10.1016/j.jhazmat.2023.132378.

[15] M. Ateia, A. Maroli, N. Tharayil, T. Karanfil, The overlooked short- and ultrashort-chain poly- and perfluorinated substances: A review, Chemosphere 220 (2019) 866–882, https://doi.org/10.1016/j.chemosphere.2018.12.186.

[16] S.J. Chow, H.C. Croll, N. Ojeda, J. Klamerus, R. Capelle, J. Oppenheimer, J. G. Jacangelo, K.J. Schwab, C. Prasse, Comparative investigation of PFAS adsorption onto activated carbon and anion exchange resins during long-term operation of a pilot treatment plant, Water Res. 226 (2022) 119198, https://doi.org/10.1016/j.watres.2022.119198.

[17] C.C. Murray, R.E. Marshall, C.J. Liu, H. Vatankhah, C.L. Bellona, PFAS treatment with granular activated carbon and ion exchange resin: Comparing chain length, empty bed contact time, and cost, J. Water Process Eng. 44 (2021) 102342, https://doi.org/10.1016/j.jwpe.2021.102342.

[18] F. Dixit, B. Barbeau, S.G. Mostafavi, M. Mohseni, Removal of legacy PFAS and other fluorotelomers: Optimized regeneration strategies in DOM-rich waters, Water Res. 183 (2020) 116098, https://doi.org/10.1016/j.watres.2020.116098.

[19] F.A. Zeidabadi, E.B. Esfahani, M. Mohseni, Effects of water matrix on per- and polyfluoroalkyl substances (PFAS) treatment: Physical-separation and degradation processes – A review, Journal of Hazardous Materials Advances 10 (2023) 100322, https://doi.org/10.1016/j.hazadv.2023.100322.

[20] E. Gagliano, M. Sgroi, P.P. Falciglia, F.G.A. Vagliasindi, P. Roccaro, Removal of poly- and perfluoroalkyl substances (PFAS) from water by adsorption: Role of PFAS chain length, effect of organic matter and challenges in adsorbent regeneration, Water Res. 171 (2020) 115381, https://doi.org/10.1016/j.watres.2019.115381.

[21] J. Wang, Z.-W. Lin, W.R. Dichtel, D.E. Helbling, Perfluoroalkyl acid adsorption by styrenic β-cyclodextrin polymers, anion-exchange resins, and activated carbon is inhibited by matrix constituents in different ways, Water Res. 260 (2024) 121897, https://doi.org/10.1016/j.watres.2024.121897.

[22] Z.-W. Lin, E.F. Shapiro, F.J. Barajas-Rodriguez, A. Gaisin, M. Ateia, J. Currie, D. E. Helbling, R. Gwinn, A.I. Packman, W.R. Dichtel, Trace Organic Contaminant Removal from Municipal Wastewater by Styrenic β-Cyclodextrin Polymers, Environ. Sci. Tech. (2023), https://doi.org/10.1021/acs.est.3c04233.

[23] E. Kumarasamy, I.M. Manning, L.B. Collins, O. Coronell, F.A. Leibfarth, Ionic Fluorogels for Remediation of Per- and Polyfluorinated Alkyl Substances from Water, ACS Cent. Sci. 6 (4) (2020) 487–492, https://doi.org/10.1021/acscentsci.9b01224.

[24] R. Wang, Z.-W. Lin, M.J. Klemes, M. Ateia, B. Trang, J. Wang, C. Ching, D. E. Helbling, W.R. Dichtel, A Tunable Porous β-Cyclodextrin Polymer Platform to Understand and Improve Anionic PFAS Removal, ACS Cent. Sci. 8 (5) (2022) 663–669, https://doi.org/10.1021/acscentsci.2c00478.

[25] Z.-W. Lin, J Wang, Y. Dyakiv, D.E. Helbling, W.R. Dichtel, Structural Features of Styrene-Functionalized Cyclodextrin Polymers That Promote the Adsorption of Perfluoroalkyl Acids in Water, ACS Appl. Mater. Interfaces (2024), https://doi.org/10.1021/acsami.4c01969.

[26] I.M. Manning, N. Guan Pin Chew, H.P. Macdonald, K.E. Miller, M.J. Strynar, O. Coronell, F.A. Leibfarth, Hydrolytically Stable Ionic Fluorogels for High-Performance Remediation of Per-and Polyfluoroalkyl Substances (PFAS) from Natural Water, Angewandte Chemie 134(41) (2022) e202208150. doi: 10.1002/anie.202208150.

[27] C. Liu, X. Zhao, A.F. Faria, K.Y. Deliz Quiñones, C. Zhang, Q. He, J. Ma, Y. Shen, Y. Zhi, Evaluating the efficiency of nanofiltration and reverse osmosis membrane processes for the removal of per- and polyfluoroalkyl substances from water: a critical review, Sep. Purif. Technol. 302 (2022) 122161, https://doi.org/10.1016/j.seppur.2022.122161.

[28] D.G. Wahman, S.J. Smith, E.J. Kleiner, G. Abulikemu, E.K. Stebel, B.N. Gray, B. C. Crone, R.D. Taylor, E.A. Womack, C.X. Gastaldo, T.T. Sanan, J.G. Pressman, L. M. Haupert, Strong Base Anion Exchange Selectivity of Nine Perfluoroalkyl Chemicals Relevant to Drinking Water, ACS ES&T Water 3 (12) (2023) 3967–3979, https://doi.org/10.1021/acsestwater.3c00396.

[29] Y. Ling, D.M. Alzate-Sánchez, M.J. Klemes, W.R. Dichtel, D.E. Helbling, Evaluating the effects of water matrix constituents on micropollutant removal by activated carbon and β-cyclodextrin polymer adsorbents, Water Res. 173 (2020) 115551, https://doi.org/10.1016/j.watres.2020.115551.

[30] C. Wu, M.J. Klemes, B. Trang, W.R. Dichtel, D.E. Helbling, Exploring the factors that influence the adsorption of anionic PFAS on conventional and emerging adsorbents in aquatic matrices, Water Res. 182 (2020) 115950, https://doi.org/10.1016/j.watres.2020.115950.

[31] B.A. Ulrich, E.A. Im, D. Werner, C.P. Higgins, Biochar and Activated Carbon for Enhanced Trace Organic Contaminant Retention in Stormwater Infiltration Systems, Environ. Sci. Tech. 49 (10) (2015) 6222–6230, https://doi.org/10.1021/acs.est.5b00376.

[32] J. Yu, L. Lv, P. Lan, S. Zhang, B. Pan, W. Zhang, Effect of effluent organic matter on the adsorption of perfluorinated compounds onto activated carbon, J. Hazard. Mater. 225–226 (2012) 99–106, https://doi.org/10.1016/j.jhazmat.2012.04.073.

[33] X. Lei, L. Yao, Q. Lian, X. Zhang, T. Wang, W. Holmes, G. Ding, D.D. Gang, M. E. Zappi, Enhanced adsorption of perfluorooctanoate (PFOA) onto low oxygen content ordered mesoporous carbon (OMC): Adsorption behaviors and mechanisms, J. Hazard. Mater. 421 (2022) 126810, https://doi.org/10.1016/j.jhazmat.2021.126810.

[34] K. Arola, B. Van der Bruggen, M. Mänttäri, M. Kallioinen, Treatment options for nanofiltration and reverse osmosis concentrates from municipal wastewater

treatment: A review, Crit. Rev. Environ. Sci. Technol. 49 (22) (2019) 2049–2116, https://doi.org/10.1080/10643389.2019.1594519.

[35] V.J. Inglezakis, M.M. Fyrillas, J. Park, Variable diffusivity homogeneous surface diffusion model and analysis of merits and fallacies of simplified adsorption kinetics equations, J. Hazard. Mater. 367 (2019) 224–245, https://doi.org/10.1016/j.jhazmat.2018.12.023.

[36] Y. Xiao, J. Azaiez, J.M. Hill, Erroneous Application of Pseudo-Second-Order Adsorption Kinetics Model: Ignored Assumptions and Spurious Correlations, Ind. Eng. Chem. Res. 57 (7) (2018) 2705–2709, https://doi.org/10.1021/acs.iecr.7b04724.

[37] A.H. Karoyo, L.D. Wilson, Nano-Sized Cyclodextrin-Based Molecularly Imprinted Polymer Adsorbents for Perfluorinated Compounds—A Mini-Review, Nanomaterials (2015) 981–1003.

[38] E.M.M. Del Valle, Cyclodextrins and their uses: a review, Process Biochem. 39 (9) (2004) 1033–1046, https://doi.org/10.1016/S0032-9592(03)00258-9.

[39] Z. Du, S. Deng, Y. Bei, Q. Huang, B. Wang, J. Huang, G. Yu, Adsorption behavior and mechanism of perfluorinated compounds on various adsorbents—A review, J. Hazard. Mater. 274 (2014) 443–454, https://doi.org/10.1016/j.jhazmat.2014.04.038.

[40] A. Yang, C. Ching, M. Easler, D.E. Helbling, W.R. Dichtel, Cyclodextrin Polymers with Nitrogen-Containing Tripodal Crosslinkers for Efficient PFAS Adsorption, ACS Mater. Lett. 2 (9) (2020) 1240–1245, https://doi.org/10.1021/acsmaterialslett.0c00240.

[41] H. Yu, H. Chen, B. Fang, H. Sun, Sorptive removal of per- and polyfluoroalkyl substances from aqueous solution: Enhanced sorption, challenges and perspectives, Sci. Total Environ. 861 (2023) 160647, https://doi.org/10.1016/j.scitotenv.2022.160647.

[42] N. Saeidi, A. Lai, F. Harnisch, G. Sigmund, A FAIR comparison of activated carbon, biochar, cyclodextrins, polymers, resins, and metal organic frameworks for the adsorption of per- and polyfluorinated substances, Chem. Eng. J. (2024) 155456, https://doi.org/10.1016/j.cej.2024.155456.

[43] Y. He, X. Cheng, S.J. Gunjal, C. Zhang, Advancing PFAS Sorbent Design: Mechanisms, Challenges, and Perspectives, ACS Mater. Au (2023), https://doi.org/10.1021/acsmaterialsau.3c00066.

[44] J. Szejtli, Introduction and General Overview of Cyclodextrin Chemistry, Chem. Rev. 98 (5) (1998) 1743–1754, https://doi.org/10.1021/cr970022c.

[45] M.J. Weiss-Errico, K.E. O'Shea, Detailed NMR investigation of cyclodextrin-perfluorinated surfactant interactions in aqueous media, J. Hazard. Mater. 329 (2017) 57–65, https://doi.org/10.1016/j.jhazmat.2017.01.017.

[46] R. Wang, C. Ching, W.R. Dichtel, D.E. Helbling, Evaluating the Removal of Per- and Polyfluoroalkyl Substances from Contaminated Groundwater with Different Adsorbents Using a Suspect Screening Approach, Environ. Sci. Technol. Lett. 7 (12) (2020) 954–960, https://doi.org/10.1021/acs.estlett.0c00736.

[47] C. Ching, M.J. Klemes, B. Trang, W.R. Dichtel, D.E. Helbling, β-Cyclodextrin Polymers with Different Cross-Linkers and Ion-Exchange Resins Exhibit Variable Adsorption of Anionic, Zwitterionic, and Nonionic PFASs, Environmental Science & Technology 54 (19) (2020) 12693–12702, https://doi.org/10.1021/acs.est.0c04028.

[48] S.C.E. Leung, D. Wanninayake, D. Chen, N.-T. Nguyen, Q. Li, Physicochemical properties and interactions of perfluoroalkyl substances (PFAS)-Challenges and opportunities in sensing and remediation, Sci. Total Environ. 166764 (2023).

[49] C. Liu, X. Zhao, A.F. Faria, K.Y.D. Quiñones, C. Zhang, Q. He, J. Ma, Y. Shen, Y. Zhi, Evaluating the efficiency of nanofiltration and reverse osmosis membrane processes for the removal of per-and polyfluoroalkyl substances from water: A critical review, Sep. Purif. Technol. 302 (2022) 122161.

[50] Y. He, X. Cheng, S.J. Gunjal, C. Zhang, Advancing PFAS Sorbent Design: Mechanisms, Challenges, and Perspectives, ACS Mater. Au 4 (2) (2023) 108–114.

[51] H. Heidari, T. Abbas, Y.S. Ok, D.C.W. Tsang, A. Bhatnagar, E. Khan, GenX is not always a better fluorinated organic compound than PFOA: A critical review on aqueous phase treatability by adsorption and its associated cost, Water Res. 205 (2021) 117683, https://doi.org/10.1016/j.watres.2021.117683.

[52] T.H. Boyer, Y. Fang, A. Ellis, R. Dietz, Y.J. Choi, C.E. Schaefer, C.P. Higgins, T. J. Strathmann, Anion exchange resin removal of per- and polyfluoroalkyl substances (PFAS) from impacted water: A critical review, Water Res. 200 (2021) 117244, https://doi.org/10.1016/j.watres.2021.117244.

[53] M. Vakili, G. Cagnetta, S. Deng, W. Wang, Z. Gholami, F. Gholami, W. Dastyar, A. Mojiri, L. Blaney, Regeneration of exhausted adsorbents after PFAS adsorption: a critical review, J. Hazard. Mater. (2024) 134429, https://doi.org/10.1016/j.jhazmat.2024.134429.

[54] M. Ateia, A. Alsbaiee, T. Karanfil, W. Dichtel, Efficient PFAS Removal by Amine-Functionalized Sorbents: Critical Review of the Current Literature, Environ. Sci. Technol. Lett. 6 (12) (2019) 688–695, https://doi.org/10.1021/acs.estlett.9b00659.